Published in IET Systems Biology
Received on 21st June 2011
Revised on 16th November 2011
doi: 10.1049/iet-syb.2011.0038

Special Issue: Modelling Noise in Biochemical Reaction Networks

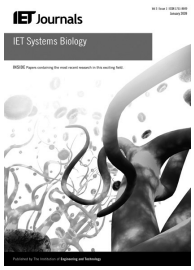

ISSN 1751-8849

Linear noise approximation is valid over limited times for any chemical system that is sufficiently large

E.W.J. Wallace[1,2] *D.T. Gillespie*[3] *K.R. Sanft*[4] *L.R. Petzold*[4]

[1]*Department of Biochemistry and Molecular Biology, University of Chicago, Chicago, IL 60637, USA*
[2]*FAS Centre for Systems Biology, Harvard University, Cambridge, MA 02138, USA*
[3]*Dan T Gillespie Consulting, 30504 Cordoba Pl., Castaic, CA 91384, USA*
[4]*Department of Computer Science, University of California Santa Barbara, Santa Barbara, CA 93106, USA*
E-mail: gillespiedt@mailaps.org

Abstract: The linear noise approximation (LNA) is a way of approximating the stochastic time evolution of a well-stirred chemically reacting system. It can be obtained either as the lowest order correction to the deterministic chemical reaction rate equation (RRE) in van Kampen's system-size expansion of the chemical master equation (CME), or by linearising the two-term-truncated chemical Kramers-Moyal equation. However, neither of those derivations sheds much light on the validity of the LNA. The problematic character of the system-size expansion of the CME for some chemical systems, the arbitrariness of truncating the chemical Kramers-Moyal equation at two terms, and the sometimes poor agreement of the LNA with the solution of the CME, have all raised concerns about the validity and usefulness of the LNA. Here, the authors argue that these concerns can be resolved by viewing the LNA as an approximation of the chemical Langevin equation (CLE). This view is already implicit in Gardiner's derivation of the LNA from the truncated Kramers-Moyal equation, as that equation is mathematically equivalent to the CLE. However, the CLE can be more convincingly derived in a way that does not involve either the truncated Kramers-Moyal equation or the system-size expansion. This derivation shows that the CLE will be valid, at least for a limited span of time, for any system that is sufficiently close to the thermodynamic (large-system) limit. The relatively easy derivation of the LNA from the CLE shows that the LNA shares the CLE's conditions of validity, and it also suggests that what the LNA really gives us is a description of the initial departure of the CLE from the RRE as we back away from the thermodynamic limit to a large but finite system. The authors show that this approach to the LNA simplifies its derivation, clarifies its limitations, and affords an easier path to its solution.

1 Introduction

The chemical master equation (CME) describes the discrete-stochastic time evolution of the molecular populations in any well-stirred chemically reacting system. In the limit of an infinitely large system, the CME reduces to the reaction rate equation (RRE), the set of ordinary differential equations that has long been the cornerstone of deterministic chemical kinetics. Proposed proofs of that limit result have used a variety of arguments [1–7], the best known of which is the 'system-size expansion' of van Kampen [4, 5]. In the system-size expansion, the solution of the CME is, in effect, expanded about the solution of the RRE in a power series in the reciprocal of the square root of the size of the system. Including only the next term in this expansion yields what has come to be known as the linear noise approximation (LNA) [4, 5]. The expansion aims not only to establish the fact of the limit, but also to provide a systematic means of computing increasingly accurate solutions of the CME by adding perturbation terms to the solution of the RRE. However, this goal can be achieved only if the coefficients of the successive terms in the series expansion are well behaved. That this is not always the case can be illustrated by two examples.

The first is a bistable chemical system whose stable states s_1 and s_2 are separated by an unstable state u so that $s_1 < u < s_2$. The RRE implies that this system will asymptotically approach s_1 if the initial state $s_0 < u$, or s_2 if $s_0 > u$. However, the CME implies that the system will perpetually visit both stable states, fluctuating around each s_i within some average range σ_i for some average time τ_i before randomly transitioning to the other stable state. Clearly it will not be possible to represent those random transitions between the stable states as any kind of perturbation to the constant stable-state value predicted by the RRE. However, this failure of the system-size expansion does not invalidate the prediction that the solution of the CME approaches the solution of the RRE in the large-system limit. That is because the CME also predicts that, in the limit of an infinitely large system, $\sigma_i/s_i \to 0$ and $\tau_i \to \infty$; thus, on any realistic time scale, the system's behaviour will appear just as described by the RRE.

A second counter-example is provided by any limit-cycle oscillator, such as, for example, the Brusselator [8, 9], or the Wilson–Cowan equations of neural dynamics [10]. In the case of the Brusselator, the RRE predicts that the molecular populations $x_1(t)$ and $x_2(t)$ of its two time-varying species will evolve in such a way that the state

point $(x_1(t), x_2(t))$ eventually traces out in the x_1–x_2 plane a closed curve C (the limit cycle curve) with a fixed period T. However, the solution to the CME asymptotically approaches a time-independent crater over the x_1–x_2 plane whose ridge is the curve C. That happens because each trajectory, starting out at a given location on C, undergoes fluctuations about the RRE prediction, and although fluctuations normal to the limit cycle will tend to be corrected, fluctuations tangential to the limit cycle will accumulate. After a sufficiently long time, it will be impossible to predict the phase of any particular trajectory. Clearly, it would be folly to try represent the stationary crater predicted by the CME as a perturbation to the regularly orbiting point predicted by the RRE. However, the distribution of an ensemble of trajectories starting at the same location will relax from the sharp peak predicted by the RRE at a rate which is, roughly, inversely proportional to the system size. Thus, by taking the species populations to be sufficiently large, the time required for the solution of the CME to relax from a sharp peak orbiting C with a fixed period to the asymptotic time-stationary crater can be made so large that deviations from the behaviour predicted by the RRE will be practically imperceptible over practical time spans.

The LNA, which includes only the lowest order correction to the RRE, has been applied by many workers in a variety of practical contexts [11–16]; fewer workers have made use of higher order perturbation terms [17–23]. An alternate way of obtaining the LNA starts with the chemical Kramers-Moyal equation, which can be derived by formally expanding selected terms on the right side of the CME in a Taylor series [5, 6]. If one truncates that expansion at two terms, one obtains an equation of the Fokker-Planck form. A linearisation of that equation about the solution of the RRE gives the LNA [6]. The problem with that derivation of the LNA is that it does not tell us the conditions under which a two-term truncation of the Kramers-Moyal equation should be acceptable. In a recent study by Ferm *et al.* [24], the LNA was applied to several specific systems with mixed results. In some cases the LNA provided an accurate approximation to the CME, but in other cases the LNA was found to be very inaccurate. Against this background, questions about the validity and practical usefulness of the LNA have arisen.

In this study, we will argue that the LNA can play a useful though carefully circumscribed role in analysing chemical systems in which stochasticity is important. However, to fully appreciate that role, it is necessary to approach the LNA in a new way. The context of this new approach to the LNA is a relatively new proof of the result that the CME becomes equivalent to the RRE in the large system limit [7]. This proof does not rely on either the system-size expansion or a truncation of the Kramers-Moyal equation, and it makes clear what the practical restrictions on the result are. In Section 2, we review this proof, and in the process establish our notation. In Section 3, we show how, from an intermediate result of that proof called the chemical Langevin equation (CLE), the LNA emerges surprisingly easily through a well-motivated approximation. (The CLE is mathematically equivalent to the two-term truncated Kramers-Moyal equation mentioned earlier, but our derivation of the CLE does not make use of that fact.) In Section 4 and the Appendix, we note that an additional advantage of this way of deriving the LNA is the simpler way it suggests for solving the LNA. From this perspective, we propose in Section 5 a refined role for the LNA in the study of stochastically evolving chemical systems. In Section 6, we give three numerical examples which illustrate our thesis that the LNA is valid, at least over sufficiently restricted times, for any chemical system that is sufficiently large. In Section 7, we summarise our conclusions.

2 Route from the CME to the RRE

We consider a system of N chemical species $S_1, \ldots, S_N$ whose molecules can undergo M chemical reactions $R_1, \ldots, R_M$. If the molecules of the reactant species are dilute and well-stirred inside some volume Ω, it can be shown [7, 25] that for each chemical reaction channel R_m there should exist a function a_m of $\boldsymbol{x} \equiv (x_1, \ldots, x_N)$, where x_i is the current number of molecules of species S_i, that satisfies

$$a_m(\boldsymbol{x})\,\mathrm{d}t \equiv \text{the probability that an } R_m \text{ reaction event will occur in the next infinitesimally small time interval } \mathrm{d}t \quad (m = 1, \ldots, M) \tag{1}$$

This function is called the propensity function of reaction R_m, as it quantifies the propensity of R_m to fire. Equation (1) implies that the time-dependent state vector of the system $\boldsymbol{X}(t) \equiv (X_1(t), \ldots, X_N(t))$, where $X_i(t)$ is the number of molecules of species S_i at time t, is a jump Markov process.

There are two important consequences of (1) that follow rigorously by applying the laws of probability theory. The first is the CME [26], which prescribes the time evolution of the function $P(\boldsymbol{x}, t|\boldsymbol{x}_0, t_0) \equiv$ the probability that $\boldsymbol{X}(t)$ will equal $\boldsymbol{x}$ given that $\boldsymbol{X}(t_0) = \boldsymbol{x}_0$ for any $t \geq t_0$:

$$\frac{\partial P(\boldsymbol{x}, t|\boldsymbol{x}_0, t_0)}{\partial t} = \sum_{m=1}^{M} [a_m(\boldsymbol{x} - \boldsymbol{\nu}_m)P(\boldsymbol{x} - \boldsymbol{\nu}_m, t|\boldsymbol{x}_0, t_0) - a_m(\boldsymbol{x})P(\boldsymbol{x}, t|\boldsymbol{x}_0, t_0)] \tag{2}$$

Here $\boldsymbol{\nu_m} \equiv (\nu_{1m}, \ldots, \nu_{Nm})$ is the state-change vector for reaction R_m, with ν_{im} being the change in the S_i molecular population caused by one R_m reaction. The other important rigorous consequence of (1) is the stochastic simulation algorithm (SSA) [27, 28]. It enables us to construct unbiased realisations of $\boldsymbol{X}(t)$ by successively advancing the system from its current state by exactly one reaction event. More specifically, if $\boldsymbol{X}(t) = \boldsymbol{x}$, then with $a_0(\boldsymbol{x}) \equiv \sum_{j=1}^{M} a_j(\boldsymbol{x})$, the time τ to the next reaction will be a sample of the exponential random variable with mean $a_0^{-1}(\boldsymbol{x})$, and the index m of that reaction will be a sample of the integer random variable with probability mass $a_m(\boldsymbol{x})/a_0(\boldsymbol{x})$. With τ and m chosen according to those specifications (there are several ways of doing that), the SSA advances the system from state $\boldsymbol{x}$ at time t to state $\boldsymbol{x} + \boldsymbol{\nu}_m$ at time $t + \tau$.

The journey from this discrete-stochastic CME/SSA description to the traditional continuous-deterministic description of the RRE begins with a formula that was originally proposed to speed up the SSA [29, 30]. The idea was to advance the system from state $\boldsymbol{x}$ at time t by a 'preselected' time τ which encompasses more than one reaction event. If we take care to choose the time step τ small enough that all the propensity functions remain approximately constant during τ, that is, if

$$a_m(\boldsymbol{x}) \doteq \text{constant in } [t, t + \tau), \ \forall m \quad \text{(first leap condition)} \tag{3}$$

then the state change in that step can easily be estimated. The Poisson random variable with mean $a\tau$, $\mathcal{P}(a\tau)$, can be defined

doi: 10.1049/iet-syb.2011.0038

as the number of events that will occur in a time τ given that $a\mathrm{d}t$, where a is any positive constant, is the probability that an event will occur in the next infinitesimal time $\mathrm{d}t$. This fact coupled with (1) implies that, under condition (3), the number of firings of reaction channel R_m in the next τ will be the Poisson random variable $\mathcal{P}_m(a_m(\boldsymbol{x})\tau)$. As each of those firings of R_m changes the system's state by $\boldsymbol{\nu}_m$, the state of the system at time $t+\tau$ can be computed as

$$\boldsymbol{X}(t+\tau) \doteq \boldsymbol{x} + \sum_{m=1}^{M} \mathcal{P}_m(a_m(\boldsymbol{x})\tau)\boldsymbol{\nu}_m \tag{4}$$

This is called the tau-leaping formula. Its accuracy depends solely on how well condition (3) is satisfied, because that condition alone controls how accurately the number of R_m firings in time τ can be approximated by $\mathcal{P}_m(a_m(\boldsymbol{x})\tau)$.

Although the tau-leaping formula (4) can often be used to simulate the evolution of a chemical system with acceptable accuracy faster than the SSA, our interest in (4) here is that it constitutes the first step in the journey from the CME/SSA to the RRE. The second step in that journey imposes a second condition on τ in (4), namely that τ also be large enough to satisfy

$$a_m(\boldsymbol{x})\tau \gg 1, \forall m \quad \text{(second leap condition)} \tag{5}$$

As $\langle \mathcal{P}(a_m(\boldsymbol{x})\tau)\rangle = a_m(\boldsymbol{x})\tau$, the physical import of requirement (5) is that each reaction channel will on average fire many more times than once in the next time step τ. Now, a well-known result in random variable theory is that a Poisson random variable whose mean μ is very large compared with 1 can be approximated by a normal random variable with mean μ and variance μ; in symbols, with $\mathcal{N}(\mu, \sigma^2)$ denoting the normal random variable with mean μ and variance σ^2, $\mathcal{P}(\mu) \doteq \mathcal{N}(\mu, \mu)$ whenever $\mu \gg 1$. Therefore if both leap conditions (3) and (5) are satisfied, we can use the identity $\mathcal{N}(\mu, \sigma^2) \equiv \mu + \sigma\mathcal{N}(0, 1)$ to further approximate the tau-leaping formula (4) as follows

$$\begin{aligned}
\boldsymbol{X}(t+\tau) &\doteq \boldsymbol{x} + \sum_{m=1}^{M} \mathcal{N}_m(a_m(\boldsymbol{x})\tau, a_m(\boldsymbol{x})\tau)\boldsymbol{\nu}_m \\
&\doteq \boldsymbol{x} + \sum_{m=1}^{M} \left[a_m(\boldsymbol{x})\tau + \sqrt{a_m(\boldsymbol{x})\tau}\mathcal{N}_m(0, 1)\right]\boldsymbol{\nu}_m \\
&\doteq \boldsymbol{x} + \sum_{m=1}^{M} \boldsymbol{\nu}_m a_m(\boldsymbol{x})\tau + \sum_{m=1}^{M} \boldsymbol{\nu}_m \sqrt{a_m(\boldsymbol{x})} N_m(t)\sqrt{\tau}
\end{aligned}$$

In the last line, the $N_m(t)$ comprise a set of M statistically independent temporally uncorrelated normal random variables with means 0 and variances 1. As τ here is assumed to be small enough to satisfy the first leap condition yet also large enough to satisfy the second leap condition, it has the character of a 'macroscopic infinitesimal'. As is often done in physics, we will simply denote it by $\mathrm{d}t$. Recalling that $\boldsymbol{x}$ stands for $\boldsymbol{X}(t)$, we thus conclude that

$$\begin{aligned}
\boldsymbol{X}(t+\mathrm{d}t) - \boldsymbol{X}(t) \doteq & \sum_{m=1}^{M} \boldsymbol{\nu}_m a_m(\boldsymbol{X}(t))\,\mathrm{d}t \\
& + \sum_{m=1}^{M} \boldsymbol{\nu}_m \sqrt{a_m(\boldsymbol{X}(t))} N_m(t)\,\sqrt{\mathrm{d}t}
\end{aligned} \tag{6}$$

This equation is called the chemical Langevin equation (CLE) [1–3, 31–33]. It can be shown (see for example [31]) to be mathematically equivalent to the Fokker-Planck equation that is obtained by truncating the Kramers-Moyal expansion of the CME at two terms. Owing to that mathematical equivalence, the two-term-truncated Kramers-Moyal equation can legitimately be called the chemical Fokker-Planck equation (CFPE).

Two caveats concerning the CLE (which also apply to the mathematically equivalent CFPE) should be kept in mind. First, the CLE will be valid only if the system admits a macroscopically infinitesimal time increment $\mathrm{d}t = \tau$ that satisfies both leap conditions (3) and (5). We note that it is easy to find chemical systems for which that requirement cannot be met, and for those systems the CLE (6) will not be valid.

Second, the CLE practically never accurately quantifies rarely occurring system trajectories. The reason for that is that the Poisson-to-normal approximation which we made in deriving the CLE, namely approximating $\mathcal{P}(\mu)$ by $\mathcal{N}(\mu, \mu)$ when $\mu \gg 1$, while accurate for sample values of those two random variables that are within a few standard deviations $\sqrt{\mu}$ of their means μ, will be very inaccurate for sample values in the near-zero tails of the two distributions (e.g. 10^{-10} against 10^{-20}). In the case of the Poisson random variables $\mathcal{P}_m(a_m(\boldsymbol{x})\tau)$ in the tau-leaping formula (4), those near-zero tails quantify unlikely or rarely occurring firing numbers of the reaction channels, and they in turn give rise to unlikely or rarely occurring system behaviours. As a consequence, the CLE practically always greatly underestimates the likelihood of rarely occurring events. In some situations, rarely occurring events will have little or no practical impact; for example, a rare large transient fluctuation about the mean in a unimodal distribution might be quickly forgotten. However, in other situations, a rarely occurring event can have dramatic consequences, for example, a spontaneous transition from one stable state to the other stable state in a bistable system. As the CLE misses rarely occurring events, which according to the CME/SSA will occur if we observe the system for a long enough time, we conclude that the CLE will generally be valid over 'only a limited span of time'. In other words, if both leap conditions are satisfied, the CLE will accurately describe the 'typical' behaviour of the system that would be observed over a limited span of time, but it will not accurately describe 'atypical' behaviour that would be observed over an arbitrarily long time span.

Assuming henceforth that we will be satisfied with knowing the typical behaviour of the system over a limited span of time, the following question arises: under what circumstances will both leap conditions be simultaneously satisfied, so that the above derivation will justify invoking the CLE (6)? For physically realistic propensity functions and state-change vectors, it has been proven [7] that both leap conditions will be satisfied if the system is sufficiently close to the thermodynamic limit. The thermodynamic limit is the traditional large-system limit in statistical mechanics in which the molecular populations and the containing volume Ω all approach infinity in such a way that the species concentrations

$$Z_i(t) \equiv \frac{X_i(t)}{\Omega} \tag{7}$$

stay constant (with respect to that limit, not with respect to t). The argument proving this result goes roughly as follows (see

[7] for details): first we establish as an empirical fact that, as the thermodynamic limit is approached, all physically reasonable propensity functions diverge linearly with the system size; more specifically, as the thermodynamic limit is approached

$$a_m(\boldsymbol{x}) \to \Omega\, \tilde{a}_m(\boldsymbol{z}) \quad (m = 1, \ldots, M) \tag{8}$$

where $\boldsymbol{z} \equiv \boldsymbol{x}/\Omega$ is the system size-independent concentration variable, and the functions $\tilde{a}_m$ are independent of the system size and are either the same or nearly the same as the functions a_m. Next, we observe that the first leap condition (3) can always be satisfied simply by taking τ sufficiently small. With τ thus fixed, we then get close enough to the thermodynamic limit that the replacement (8) will be justified, allowing us to write the second leap condition (5) as $\Omega\tilde{a}_m(\boldsymbol{z})\tau \gg 1$. That condition can evidently be satisfied simply by continuing far enough towards the thermodynamic limit. Thus, we conclude that, by getting close enough to the thermodynamic limit, we can satisfy both leap conditions, and thereby assure that the CLE (6) (and its companion CFPE) holds – at least over a sufficiently limited span of time.

Being close to the thermodynamic limit is not only a sufficient condition for the validity of the CLE, but also a necessary condition. That is because the time-varying molecular populations $X_i(t)$, which are discretely varying integer variables, will not look like the continuously varying real variables in the CLE unless the $X_i(t)$ are ranging over values that are $\gg 1$. It is therefore always permissible to make the large-system replacement (8) in the CLE (6). Upon doing that, and then dividing through by Ω, we obtain the 'concentration form' of the CLE

$$\begin{aligned}\boldsymbol{Z}(t + \mathrm{d}t) - \boldsymbol{Z}(t) \doteq & \sum_{m=1}^{M} \boldsymbol{\nu}_m \tilde{a}_m(\boldsymbol{Z}(t))\, \mathrm{d}t \\ & + \frac{1}{\sqrt{\Omega}} \sum_{m=1}^{M} \boldsymbol{\nu}_m \sqrt{\tilde{a}_m(\boldsymbol{Z}(t))}\, N_m(t)\, \sqrt{\mathrm{d}t}\end{aligned} \tag{9}$$

Equation (9) makes it easy to see what happens to the CLE when we finally proceed fully to the thermodynamic limit. The two terms on the left side of (9), and also the first term on the right, will all stay constant. However, the second term on the right will go to zero. Therefore in the full thermodynamic limit the CLE (9) reduces to

$$\boldsymbol{Z}(t + \mathrm{d}t) - \boldsymbol{Z}(t) = \sum_{m=1}^{M} \boldsymbol{\nu}_m \tilde{a}_m(\boldsymbol{Z}(t))\, \mathrm{d}t$$

This is equivalent to the ordinary differential equation

$$\frac{\mathrm{d}\boldsymbol{Z}(t)}{\mathrm{d}t} = \sum_{m=1}^{M} \boldsymbol{\nu}_m \tilde{a}_m(\boldsymbol{Z}(t)) \tag{10a}$$

Equation (10a) is the RRE, expressed in terms of the species concentrations. If we multiply it through by Ω and again make use of the property (8), we obtain the RRE in terms of the molecular populations

$$\frac{\mathrm{d}\boldsymbol{X}(t)}{\mathrm{d}t} = \sum_{m=1}^{M} \boldsymbol{\nu}_m a_m(\boldsymbol{X}(t)) \tag{10b}$$

In summary, if any chemical system is sufficiently close to the thermodynamic limit, its CLE will be valid for at least a limited duration of time. The closer the system is to the thermodynamic limit, the longer the CLE's duration of validity will be. And if the system is taken all the way to the thermodynamic limit, the CLE will become the RRE with an essentially infinite duration of validity – assuming, that is, that an infinitely large system can be kept well stirred.

3 Deriving the LNA

Against the background summarised in the preceding paragraph, we will now derive the LNA as an approximation to the CLE, assuming of course that the system is close enough to the thermodynamic limit that the CLE is valid. Observing that the CLE (9) differs from the RRE (10a) by a term that is proportional to $1/\sqrt{\Omega}$, we make the ansatz that the solution $\boldsymbol{Z}(t)$ to the CLE will differ from the solution $\hat{\boldsymbol{Z}}(t)$ to the RRE by a term that is likewise proportional to $1/\sqrt{\Omega}$. We note that this ansatz is essentially the same as that originally made by van Kampen [4, 5] and echoed by Gardiner [6]. We seek, therefore, a solution to the CLE (9) of the form

$$\boldsymbol{Z}(t) = \hat{\boldsymbol{Z}}(t) + \frac{1}{\sqrt{\Omega}}\boldsymbol{\xi}(t) \tag{11}$$

where $\hat{\boldsymbol{Z}}(t)$ is the deterministic function that satisfies the RRE (10a)

$$\frac{\mathrm{d}\hat{\boldsymbol{Z}}(t)}{\mathrm{d}t} = \sum_{m=1}^{M} \boldsymbol{\nu}_m \tilde{a}_m(\hat{\boldsymbol{Z}}(t)) \tag{12}$$

and also the initial condition

$$\hat{\boldsymbol{Z}}(t_0) = \boldsymbol{Z}(t_0) \tag{13}$$

To find the stochastic function $\boldsymbol{\xi}(t)$ that makes (11) a solution of (9), we begin by substituting (11) into (9) to obtain

$$\begin{aligned}&[\hat{\boldsymbol{Z}}(t + \mathrm{d}t) - \hat{\boldsymbol{Z}}(t)] + \frac{1}{\sqrt{\Omega}}[\boldsymbol{\xi}(t + \mathrm{d}t) - \boldsymbol{\xi}(t)] \\ &\quad = \sum_{m=1}^{M} \boldsymbol{\nu}_m \tilde{a}_m\left(\hat{\boldsymbol{Z}}(t) + \frac{1}{\sqrt{\Omega}}\boldsymbol{\xi}(t)\right) \mathrm{d}t \\ &\qquad + \frac{1}{\sqrt{\Omega}} \sum_{m=1}^{M} \boldsymbol{\nu}_m \sqrt{\tilde{a}_m\left(\hat{\boldsymbol{Z}}(t) + \frac{1}{\sqrt{\Omega}}\boldsymbol{\xi}(t)\right)}\, N_m(t)\, \sqrt{\mathrm{d}t}\end{aligned}$$

As $\hat{\boldsymbol{Z}}(t)$ satisfies the RRE (12), then $\hat{\boldsymbol{Z}}(t + \mathrm{d}t) - \hat{\boldsymbol{Z}}(t)$ on the left side of this equation can be replaced by $\Sigma_m \boldsymbol{\nu}_m \tilde{a}_m(\hat{\boldsymbol{Z}}(t))\, \mathrm{d}t$. Doing that, and then multiplying through by $\sqrt{\Omega}$, we obtain

$$\begin{aligned}&\boldsymbol{\xi}(t + \mathrm{d}t) - \boldsymbol{\xi}(t) \\ &\quad = \sqrt{\Omega} \sum_{m=1}^{M} \boldsymbol{\nu}_m \left[\tilde{a}_m\left(\hat{\boldsymbol{Z}}(t) + \frac{1}{\sqrt{\Omega}}\boldsymbol{\xi}(t)\right) - \tilde{a}_m(\hat{\boldsymbol{Z}}(t))\right] \mathrm{d}t \\ &\qquad + \sum_{m=1}^{M} \boldsymbol{\nu}_m \sqrt{\tilde{a}_m\left(\hat{\boldsymbol{Z}}(t) + \frac{1}{\sqrt{\Omega}}\boldsymbol{\xi}(t)\right)}\, N_m(t)\, \sqrt{\mathrm{d}t}\end{aligned} \tag{14}$$

This is the equation that $\boldsymbol{\xi}(t)$ must satisfy in order for $\boldsymbol{Z}(t)$ in (11) to exactly satisfy the CLE (9). However, as we are near the

doi: 10.1049/iet-syb.2011.0038

thermodynamic limit where $\boldsymbol{Z}(t) \simeq \hat{\boldsymbol{Z}}(t)$, it is reasonable to expect that the term $\boldsymbol{\xi}(t)/\sqrt{\Omega}$ in (11) will be small compared with $\hat{\boldsymbol{Z}}(t)$, thus we can make the approximation

$$\begin{aligned}\tilde{a}_m\left(\hat{\boldsymbol{Z}}(t)+\frac{1}{\sqrt{\Omega}}\boldsymbol{\xi}(t)\right) &\doteq \tilde{a}_m(\hat{\boldsymbol{Z}}(t)) \\ &\quad+\sum_{k=1}^{N}\left.\frac{\partial\tilde{a}_m(\boldsymbol{z})}{\partial z_k}\right|_{z=\hat{\boldsymbol{Z}}(t)}\left(\frac{1}{\sqrt{\Omega}}\xi_k(t)\right) \\ &\doteq \tilde{a}_m(\hat{\boldsymbol{Z}}(t))+\frac{1}{\sqrt{\Omega}}\sum_{k=1}^{N}f_{mk}(t)\xi_k(t)\end{aligned} \tag{15}$$

where in the last step we have defined the deterministic functions

$$f_{mk}(t)\equiv\left.\frac{\partial\tilde{a}_m(\boldsymbol{z})}{\partial z_k}\right|_{z=\hat{\boldsymbol{Z}}(t)} \quad (m=1,\ \ldots,M;\ k=1,\ \ldots,N) \tag{16}$$

Substituting (15) into (14), and then discarding all terms in $1/\sqrt{\Omega}$ of order ≥ 1, as the approximation (15) implicitly requires us to do, we finally obtain

$$\begin{aligned}\boldsymbol{\xi}(t+\mathrm{d}t)-\boldsymbol{\xi}(t) &\doteq \sum_{k=1}^{N}\left(\sum_{m=1}^{M}\boldsymbol{\nu}_m f_{mk}(t)\right)\xi_k(t)\,\mathrm{d}t \\ &\quad+\sum_{m=1}^{M}\boldsymbol{\nu}_m\sqrt{\tilde{a}_m(\hat{\boldsymbol{Z}}(t))}N_m(t)\,\sqrt{\mathrm{d}t}\end{aligned} \tag{17}$$

Equation (17) is van Kampen's LNA [4, 5]. In view of the definition (11) and the initial condition (13), (17) is to be solved subject to the initial condition

$$\boldsymbol{\xi}(t_0)=0 \tag{18}$$

Although the LNA (17) might appear to be more complicated than the CLE (9) which it approximates, the LNA is in one important respect simpler: its stochastic term is independent of the process that it defines. That is not true of the CLE (9), nor of the mathematically equivalent (14).

We should comment here on the connection between the foregoing derivation of the LNA to both van Kampen's original derivation [4, 5] and Gardiner's later derivation [6]. As mentioned earlier, the ansatz (11) is common to all. However, van Kampen applied that ansatz to the CME, not to the CLE as we have done here. In addition, he inferred the LNA by expanding both sides of the CME in a Taylor series about $\hat{\boldsymbol{Z}}(t)$ and then equating terms of equal order in $1/\sqrt{\Omega}$. Although the tactic of equating terms of the same order in an expansion parameter is common in analysis, the mathematical justification for doing that here is not completely clear, because the set of power functions $\{1, x, x^2, x^3 \ldots\}$ is not orthogonal. In any case, there is no assurance that the resulting series expansion will be well behaved, as apparently it is not in the two examples described in Section 1. Our derivation of the LNA from the CLE avoids those difficulties, and has the additional advantage of being simpler. Of course, we have not derived van Kampen's full system-size expansion; indeed, the only way to do that is to follow van Kampen and apply the ansatz (11) directly to the CME. However, it was not our objective here to derive the system-size expansion; our objective was to derive the CLE/CFPE, the LNA and the RRE independently of that sometimes ill-conditioned expansion.

Our derivation of the LNA is more in line with Gardiner's derivation [6], which linearised the two-term-truncated Kramers-Moyal expansion of the CME. As that two-term-truncated Kramers-Moyal equation turns out to be mathematically equivalent to the CLE (6), linearising one is mathematically equivalent to linearising the other. However, although Gardiner simply assumed the validity of the truncated Kramers-Moyal equation, we derived the CLE via a series of physically transparent approximations which showed under what conditions the CLE (and hence the mathematically equivalent CFPE) should be valid. Conveniently, fewer mathematical manipulations are required to linearise the CLE than the CFPE.

4 Solution of the LNA

The solution of the LNA (17) is known [4–6]: each component $\xi_i(t)$ of $\boldsymbol{\xi}(t)$ is a normal random variable with mean zero and variance $\kappa_{ii}(t)$

$$\xi_i(t)\doteq\mathcal{N}(0,\ \kappa_{ii}(t)) \quad (i=1,\ \ldots,N) \tag{19}$$

and is statistically dependent on the other components through the covariances

$$\mathrm{cov}\{\xi_i(t),\ \xi_j(t)\}=\langle\xi_i(t)\xi_j(t)\rangle\equiv\kappa_{ij}(t) \quad (i,j=1,\ \ldots,N) \tag{20}$$

Here the (deterministic) functions $\kappa_{ij}(t)$ are the solutions of the set of coupled, linear, ordinary differential equations

$$\begin{aligned}\frac{\mathrm{d}\kappa_{ij}(t)}{\mathrm{d}t} &\doteq \sum_{k=1}^{N}\left(\sum_{m=1}^{M}\nu_{im}f_{mk}(t)\right)\kappa_{kj}(t) \\ &\quad+\sum_{k=1}^{N}\left(\sum_{m=1}^{M}\nu_{jm}f_{mk}(t)\right)\kappa_{ki}(t) \\ &\quad+\sum_{m=1}^{M}\nu_{im}\nu_{jm}\,\tilde{a}_m(\hat{\boldsymbol{Z}}(t)) \quad (i,j=1,\ \ldots,N)\end{aligned} \tag{21}$$

for the initial conditions

$$\kappa_{ij}(t_0)=0 \quad (i,j=1,\ \ldots,N) \tag{22}$$

where $f_{mk}(t)$ is as defined in (16), and $\hat{\boldsymbol{Z}}(t)$ is the solution of the RRE (12). As any set of normal random variables is completely determined by their means, variances and covariances, the above constitutes a complete characterisation of the solution $\boldsymbol{\xi}(t)$ of the LNA (17).

Heretofore, the customary way of obtaining the above results [5, 6] was to solve the Fokker-Planck equation corresponding to the Langevin (17). In the Appendix, we show how the solution follows directly from (17).

5 LNA describes incipient stochastic behaviour near the thermodynamic limit

In Section 2 we proved, without invoking the system-size expansion or making a summary truncation of the Kramers-Moyal equation, that any realistic chemical system which is sufficiently close to the thermodynamic limit will

be accurately described, at least for limited time spans, by the CLE, and in the full thermodynamic limit by the RRE. To the question of how large a system must be in order for the CLE or the RRE to produce 'acceptable' results, no general answer can be given apart from a post-facto comparison of simulated CLE or RRE trajectories with SSA trajectories. The answer will depend not only on the topology of the reaction network, but also on the values of the reaction rates. There is, however, another less formidable question in this vein that we could pose. Suppose we start with the system effectively at the thermodynamic limit, and hence well described by its RRE, and then gradually move the system towards a finite but still large size. What will be the first noticeable stochastic departures from the deterministic behaviour predicted by the RRE?

This less ambitious question can be answered by the LNA, as it essentially mediates between the CLE and the RRE. By combining the result (19) with the solution (11) to the CLE (9), we may conclude that the incipient stochastic behaviour of the concentration of species S_i is $Z_i(t) \doteq \hat{Z}_i(t) + \Omega^{-1/2} \times \mathcal{N}(0, \kappa_{ii}(t))$, or equivalently

$$Z_i(t) \doteq \mathcal{N}(\hat{Z}_i(t), \Omega^{-1}\kappa_{ii}(t)) \quad (i = 1, \ldots, N) \tag{23}$$

Here, $\kappa_{ii}(t)$ is part of the solution to (21) for the initial condition (22). In words, as we back off from an infinitely large system to a finite system, the initial break from the purely deterministic behaviour of the RRE (13) will be normal random fluctuations in the concentrations of species S_i about the RRE values $\hat{Z}_i(t)$ with standard deviations $\sqrt{\kappa_{ii}(t)/\Omega}$. Therefore as we move towards the thermodynamic limit, the sizes of the fluctuations in the concentrations will decrease in proportion to $\sqrt{1/\Omega}$. Multiplying (23) through by Ω gives us the population version of this result

$$X_i(t) \doteq \mathcal{N}(\hat{X}_i(t), \Omega\,\kappa_{ii}(t)) \quad (i = 1, \ldots, N) \tag{24}$$

This says that the incipient stochastic behaviour will manifest itself as normal random fluctuations in the populations of species S_i about the RRE values $\hat{X}_i(t)$ with standard deviations $\sqrt{\Omega\,\kappa_{ii}(t)}$. Therefore as we move toward the thermodynamic limit, the sizes of the fluctuations in the populations will increase in proportion to $\sqrt{\Omega}$, whereas the populations themselves will of course increase (more rapidly) in proportion to Ω.

To see what is implied by the covariances $\kappa_{ij}(t)$ for $i \neq j$, we will make use of the easily proved identity

$$\mathrm{cov}\{(a_1 + b_1 Y_1), (a_2 + b_2 Y_2)\} = b_1 b_2 \mathrm{cov}\{Y_1, Y_2\}$$

Applying this identity to (11), and then making use of the definition (20), we find that the covariance of the S_i concentration with the S_j concentration is

$$\begin{aligned} \mathrm{cov}\{Z_i(t), Z_j(t)\} &= (\Omega^{-1/2})^2 \mathrm{cov}\{\xi_i(t), \xi_j(t)\} \\ &\doteq \Omega^{-1}\kappa_{ij}(t) \end{aligned} \tag{25a}$$

And multiplying this result through by Ω^2 gives for the species populations

$$\mathrm{cov}\{X_i(t), X_j(t)\} \doteq \Omega\,\kappa_{ij}(t) \tag{25b}$$

A more revealing indicator of the degree of coupling between any two random variables X and Y than their covariance is their correlation,

$$\mathrm{corr}\{X, Y\} \equiv \frac{\mathrm{cov}\{X, Y\}}{\sqrt{\mathrm{var}\{X\}\mathrm{var}\{Y\}}}$$

The correlation is a dimensionless number between -1 and $+1$, with the value $+1$ implying that X and Y are perfectly correlated (as would be the case if $Y = X$), the value -1 implying that X and Y are perfectly anti-correlated (as would be the case if $Y = -X$), and the value 0 implying that X and Y are uncorrelated. It follows from Eqs. (25) that

$$\mathrm{corr}\{X_i(t), X_j(t)\} = \mathrm{corr}\{Z_i(t), Z_j(t)\} \doteq \frac{\kappa_{ij}(t)}{\sqrt{\kappa_{ii}(t)\kappa_{jj}(t)}} \tag{26}$$

The fact that correlation (26) is independent of Ω carries a rather surprising conclusion. The correlation between the populations (or concentrations) of any two species in the LNA is exactly the same as it is in the full thermodynamic limit where the RRE applies. Therefore as we back off from the full thermodynamic limit, the only initial indicator of the finiteness of the system will be the normal fluctuations of the individual species about their RRE means with the variances given in (23) and (24).

To make practical use of the LNA, we need two things. First, we need a general purpose computer program to solve the RRE (12) for a given chemical system. It could be argued that that should always be done as a first step towards understanding the given system. Second, we need a general purpose computer program to solve the differential equation (21) for the $\kappa_{ij}(t)$, making use of the solution to the RRE (12). In that regard, notice that equations (21) are not as complicated as they might at first appear. Although they are coupled, they are linear. In addition, the fact that the concentration propensity functions $\tilde{a}_m(\boldsymbol{z})$ are usually either linear or quadratic in the components of $\boldsymbol{z}$ means that the quantities $f_{mj}(t)$ in (21), which are defined in (16), will usually be either constant or linear in a single component of $\boldsymbol{z}$.

If the system is stable, in that the solution of the RRE (12) has a well-defined, time-independent asymptotic limit

$$\hat{\boldsymbol{Z}}(t \to \infty) = \hat{\boldsymbol{Z}}(\infty) \tag{27}$$

and if we are interested only in the equilibrium behaviour of the system, then the above tasks simplify considerably. The asymptotic solution to the RRE can be found simply by solving the set of purely algebraic equations obtained by setting the left side of (12) to zero

$$\sum_{m=1}^{M} \boldsymbol{\nu}_m \tilde{a}_m(\hat{\boldsymbol{Z}}(\infty)) = 0 \tag{28}$$

And the $\kappa_{ij}(\infty)$ can be found by solving the set of purely algebraic equations obtained by setting the left side of (21) to zero

$$\begin{aligned} &\sum_{k=1}^{N}\left(\sum_{m=1}^{M}\nu_{im}f_{mk}(\infty)\right)\kappa_{kj}(\infty) + \sum_{k=1}^{N}\left(\sum_{m=1}^{M}\nu_{jm}f_{mk}(\infty)\right)\kappa_{ki}(\infty) \\ &\qquad + \sum_{m=1}^{M}\nu_{im}\nu_{jm}\,\tilde{a}_m(\hat{\boldsymbol{Z}}(\infty)) = 0 \quad (i, j = 1, \ldots, N) \end{aligned} \tag{29}$$

So at equilibrium, the earliest indication of finite-system

doi: 10.1049/iet-syb.2011.0038

effects will be normal fluctuations in the concentration of species S_i about its steady-state RRE value $\hat{Z}_i(\infty)$ with standard deviation $\sqrt{\kappa_{ii}(\infty)/\Omega}$.

6 Numerical examples

We conclude by presenting three numerical examples to illustrate our thesis that, for practical purposes, the LNA will always give a good description of any real-world chemical system that is 'sufficiently large', but not necessarily if the system is 'too small'. In these examples, the specific reaction probability rate constant c_m is defined so that $c_m \mathrm{d}t$ gives the probability that a randomly chosen set of R_m reactant molecules will react accordingly in the next dt. For real-world chemical reactions, c_m will be independent of the system volume Ω if R_m is unimolecular, inversely proportional to Ω if R_m is bimolecular, and directly proportional to Ω if R_m is a zeroth order reaction [6]. Our computations for these examples were performed using a general purpose LNA solver that was coded in C++ as a custom driver, built on top of the StochKit2 stochastic simulation software framework [34]. For the ordinary differential equations solver, the code uses CVODE from the SUNDIALS numerical software suite [35].

Example 1: Our first example is the decay-dimerisation reaction set

$$\left.\begin{array}{l} S_1 \xrightarrow{c_1} \emptyset \\ 2S_1 \underset{c_3}{\overset{k_2\Omega^{-1}}{\rightleftarrows}} S_2 \\ S_2 \xrightarrow{c_3} S_3 \end{array}\right\} \tag{30}$$

in which an unstable monomer S_1 can dimerise to an unstable dimer S_2, which in turn can convert to a stable form S_3. The state-change vectors for these four reactions are

$$\left.\begin{array}{l} \boldsymbol{\nu_1} = (-1, 0, 0) \\ \boldsymbol{\nu_2} = (-2, 1, 0) \\ \boldsymbol{\nu_3} = (2, -1, 0) \\ \boldsymbol{\nu_4} = (0, -1, 1) \end{array}\right\} \tag{31a}$$

The corresponding propensity functions are

$$\left.\begin{array}{l} a_1(\boldsymbol{x}) = c_1 x_1 \\ a_2(\boldsymbol{x}) = k_2\Omega^{-1}\frac{1}{2}x_1(x_1-1) \\ a_3(\boldsymbol{x}) = c_3 x_2 \\ a_4(\boldsymbol{x}) = c_4 x_2 \end{array}\right\} \tag{31b}$$

The Ω-independent functions defined in (8) are therefore

$$\left.\begin{array}{l} \tilde{a}_1(\boldsymbol{z}) = c_1 z_1 \\ \tilde{a}_2(\boldsymbol{z}) = k_2\frac{1}{2}z_1^2 \\ \tilde{a}_3(\boldsymbol{z}) = c_3 z_2 \\ \tilde{a}_4(\boldsymbol{z}) = c_4 z_2 \end{array}\right\} \tag{31c}$$

For the rate constant values, we will take

$$c_1 = 1, \quad k_2 = 2, \quad c_3 = 0.5, \quad c_4 = 0.04 \tag{31d}$$

and for the initial conditions

$$X_1(0) = 5 \cdot \Omega, \quad X_2(0) = X_3(0) = 0 \tag{31e}$$

By taking the initial molecular populations of all species proportional to Ω, the system can be made to approach the thermodynamic limit simply by letting $\Omega \to \infty$.

In Fig. 1, we show results for this reaction set with $\Omega = 1$, which by (31e) implies a 'small' system with only five initial S_1 molecules. Fig. 1*a* shows the mean S_2 concentration $\langle Z_2(t)\rangle$ and the corresponding one-standard deviation envelope $\langle Z_2(t)\rangle \pm \mathrm{stdev}\{Z_2(t)\}$ as a function of t, computed in two different ways: the solid and dashed curves were obtained by averaging over 10^5 SSA runs; the dotted curves are the LNA's prediction, $\hat{Z}_2(t) \pm \sqrt{\Omega^{-1}\kappa_{22}(t)}$. The step function curve in Fig. 1*a* shows a typical SSA trajectory for $Z_2(t)$. Note that concentration trajectories will always be confined to discrete values for a finite system, and in this $\Omega = 1$ case the concentration trajectory numerically coincides with the population trajectory. In Fig. 1*b*, the grey histogram shows the statistical distribution of $Z_2(t)$ at time $t = 5$ as computed from the same 10^5 SSA runs. And the solid curve shows the pdf of the LNA's prediction for this histogram, $Z_2(5) \doteq \mathcal{N}(\hat{Z}_2(5), \Omega^{-1}\kappa_{22}(5))$. We see from Figs. 1*a* and *b* that, for this 'small' system, the LNA predictions, although not wildly incorrect, differ noticeably from the exact SSA results. Even more revealing of the inaccuracy of the LNA in this case is the fact that the SSA trajectory in Fig. 1*a* is far from being a continuous (but not differentiable) curve, as the CLE and its approximating LNA both imply.

In Fig. 2, we repeat the foregoing analysis with $\Omega = 200$, which gives us an initially 'large' system with 1000 S_2 molecules. We see in Fig. 2*a* that the LNA's prediction for the one-standard deviation envelope for $Z_2(t)$ shows no discernable disagreement with the one-standard deviation envelope predicted by the 10^5 SSA runs. Note that the axes in Figs. 2*a* are identical to the axes in Fig. 1*a*. The single SSA trajectory for $Z_2(t)$ in Fig. 2*a* (jagged curve) is evidently much closer to being continuous (but not differentiable), as implied by the CLE and the LNA. In Fig. 2*b*, the S_2 concentration histogram for $Z_2(5)$ computed from 10^5 SSA runs is seen to be accurately duplicated by the pdf of the LNA's prediction, $Z_2(5) \doteq \mathcal{N}(\hat{Z}_2(5), \Omega^{-1}\kappa_{22}(5))$, which is the solid curve. The LNA for this 'large' system clearly works quite well.

Example 2: Our second example is the well-known Schlögl reaction set

$$\left.\begin{array}{l} 2S_1 \underset{k_2\Omega^{-2}}{\overset{k_1\Omega^{-1}}{\rightleftarrows}} 3S_1 \\ \emptyset \underset{c_4}{\overset{k_3\Omega}{\rightleftarrows}} S_1 \end{array}\right\} \tag{32}$$

The state-change vectors for these single-species reactions are

$$\nu_1 = 1, \quad \nu_2 = -1, \quad \nu_3 = 1, \quad \nu_4 = -1 \tag{33a}$$

and the propensity functions are

$$\left.\begin{array}{l} a_1(x_1) = k_1\Omega^{-1}\frac{1}{2}x_1(x_1-1) \\ a_2(x_1) = k_2\Omega^{-2}\frac{1}{6}x_1(x_1-1)(x_1-2) \\ a_3(x_1) = k_3\Omega \\ a_4(x_1) = c_4 x_1 \end{array}\right\} \tag{33b}$$

The volume dependence assumed here for the trimolecular

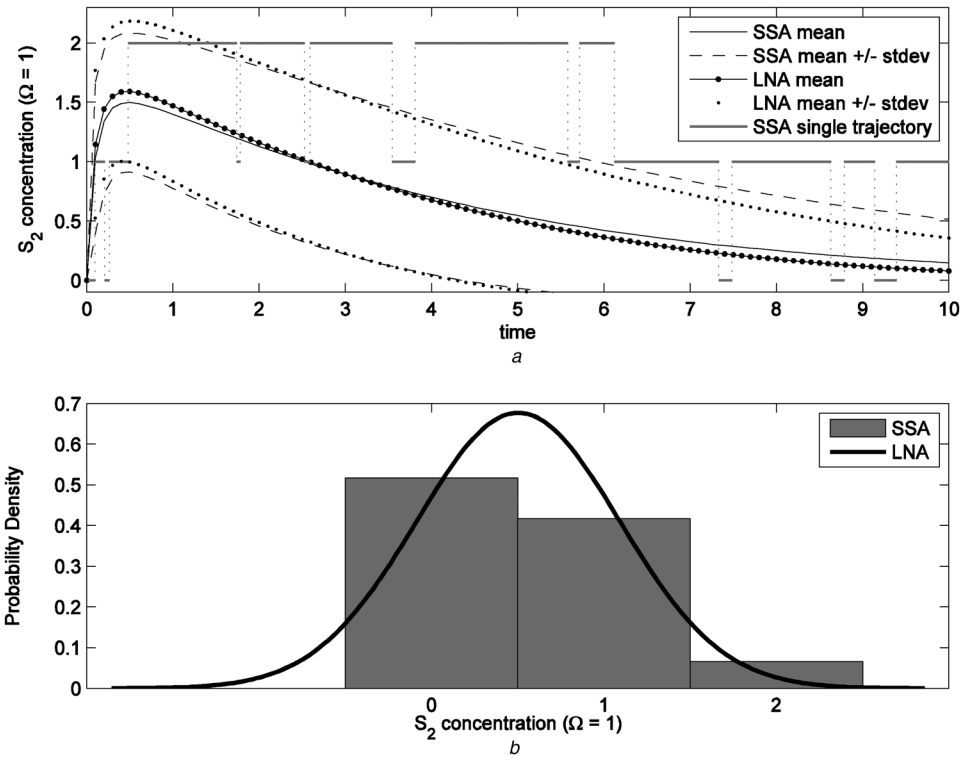

Fig. 1 *Decay-dimerisation model in (30) and (31) for $\Omega = 1$*

a Mean and mean $\pm$ one-standard deviation of the concentration of species S_2 computed from 10^5 SSA simulations (solid and dashed curves) and from the LNA (dotted curves). The grey step-curve shows a typical SSA trajectory
b Histogram of the species S_2 concentration at $t = 5$, as calculated from 10^5 SSA simulations (grey histogram), and from the LNA's normal distribution (solid curve). The LNA is evidently not accurate for this 'small' system

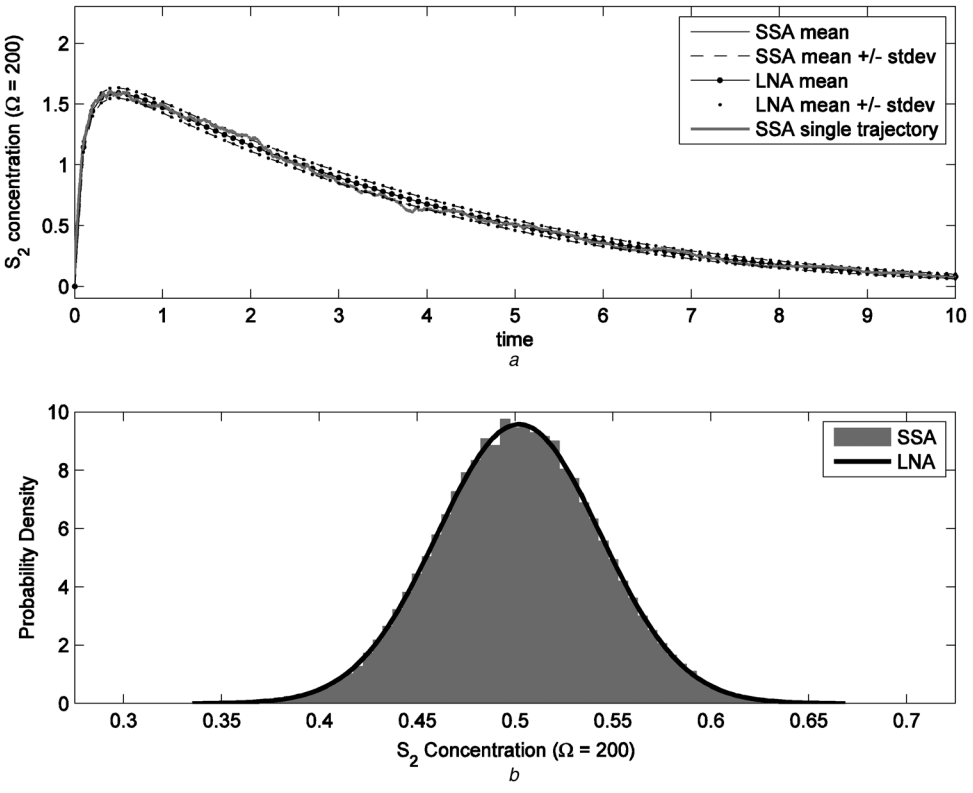

Fig. 2 *As in Fig. 1, but with $\Omega = 200$*

a LNA curves are covered by the SSA curves, and the single SSA trajectory has a more continuous appearance
b SSA histogram is accurately described by the LNA distribution. The LNA does quite well for this 'large' system

doi: 10.1049/iet-syb.2011.0038

rate constant c_2 is what arises from any physically reasonable approximation of a set of unimolecular and bimolecular reactions by a single trimolecular reaction. The Ω-independent functions defined in (8) are

$$\left.\begin{aligned}\tilde{a}_1(z_1) &= k_1\tfrac{1}{2}z_1^2\\ \tilde{a}_2(z_1) &= k_2\tfrac{1}{6}z_1^3\\ \tilde{a}_3(z_1) &= k_3\\ \tilde{a}_4(z_1) &= c_4 z_1\end{aligned}\right\} \quad (33c)$$

We take for the parameter values,

$$k_1 = 0.03, \quad k_2 = 0.0001, \quad k_3 = 200, \quad c_4 = 3.5 \quad (33d)$$

and for the initial condition

$$X_1(0) = 280 \cdot \Omega \quad (33e)$$

Fig. 3 shows numerical results for $\Omega = 1$. In Fig. 3*a*, the LNA's predictions for the one-standard deviation envelope of Z_1(t) (again shown by the dotted curves) is compared with SSA's predictions (again shown by the solid and dashed curves) over the time interval $0 \le t \le 10$. The SSA results here were again obtained from 10^5 simulation runs, and the trajectory of a randomly chosen one of those SSA runs is shown as the jagged grey curve. We see that, despite the fairly large number of S_1 molecules here (note that the population in this case is numerically equal to the concentration), the LNA performs poorly. The reason why becomes clear when we look at the corresponding predictions in Fig. 3*b* for the distribution of the S_1 concentration at time $t = 10$. The system is bi-modal, with one stable state at $z_1 = 82$ and the other at $z_2 = 563$. As the initial S_1 concentration of $z_1 = 280$ is above the separating barrier state, which happens to be at $z_b = 248$, the deterministic RRE trajectory goes to the upper stable state. However, some of the SSA trajectories ($\sim$22% in this case) wind up in the lower stable state. Thus, the LNA's prediction for the $Z_1(10)$ distribution, namely the single peak described by the solid curve, differs markedly from the SSA's double-peak prediction, shown by the grey histogram. The message here is that, over this time span, the system is not close enough to the thermodynamic limit for the LNA to accurately describe its behaviour.

However, if we increase the system volume to $\Omega = 100$, the situation changes dramatically, as shown in Fig. 4. In Fig. 4*a*, the one-standard deviation envelope predicted by the LNA is for practical purposes identical to that predicted by the SSA over the same time interval $0 \le t \le 10$. And in Fig. 4*b*, the $Z_1(10)$ distribution predicted by the LNA (solid curve) is practically indistinguishable from that predicted by the SSA (grey histogram). At this 100-fold larger system, it is extremely unlikely (though not absolutely impossible) for an SSA trajectory that starts at $z_1 = 280$ to visit the lower stable state before time $t = 10$. However, of course, if the run time here were taken to be much larger than 10, the grey SSA histogram would again become bimodal. The message here is that if a bistable system is sufficiently close to the thermodynamic limit, its behaviour over a sufficiently restricted time span will be very well described by the LNA.

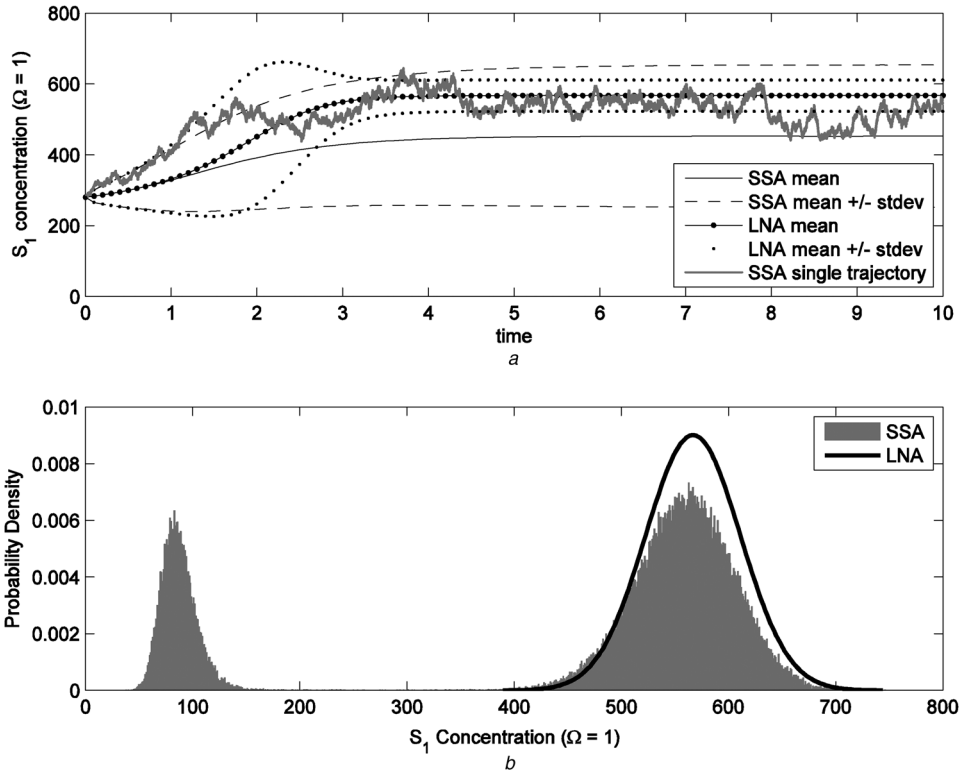

Fig. 3 *Schlögl model in (32) and (33) for $\Omega = 1$*

a Mean and mean $\pm$ one-standard deviation of the concentration of species S_1 computed from 10^5 SSA simulations (solid and dashed curves) and from the LNA (dotted curves). The jagged grey curve shows a typical SSA trajectory

b Histogram of the species S_1 concentration at $t = 10$, as calculated from 10^5 SSA simulations (grey histogram) and from the LNA's normal distribution (solid curve). The LNA is inaccurate for this 'small' bi-stable system over this long time frame

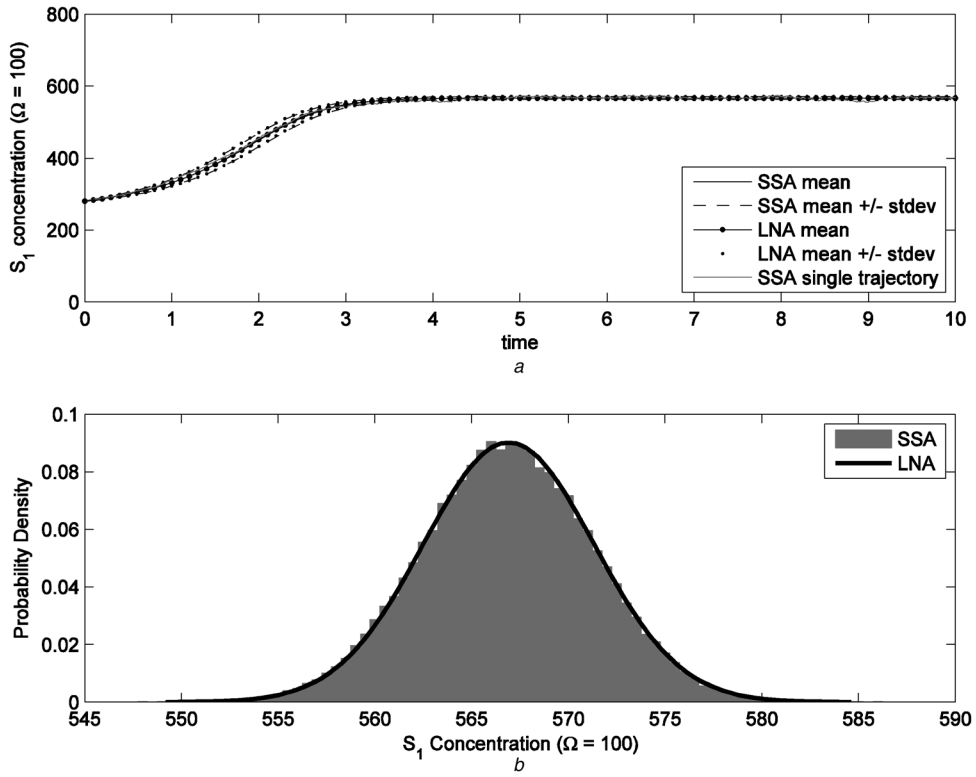

Fig. 4 *As in Fig. 3, but with $\Omega = 100$: moving closer to the thermodynamic limit allows the LNA to give a much more accurate approximation over this time frame, but over increasingly longer time frames the performance of the LNA will deteriorate*

a Mean and mean $\pm$ one-standard deviation of the concentration of species S_1 computed from 10^5 SSA simulations (solid and dashed curves) and from the LNA (dotted curves). The jagged gray curve shows a typical SSA trajectory

b Histogram of the species S_1 concentration at $t = 10$, as calculated from 10^5 SSA simulations (gray histogram) and from the LNA's normal distribution (solid curve)

Note that the x-axis in (*b*) is different from that in Fig. 3*b*, as none of these simulations reached the lower stable state

Example 3: Our final example is the famous Brusselator reaction set

$$\left.\begin{aligned} \emptyset &\xrightarrow{k_1\Omega} S_1 \\ S_1 &\xrightarrow{c_2} S_2 \\ 2S_1 + S_2 &\xrightarrow{k_3\Omega^{-2}} 3S_1 \\ S_1 &\xrightarrow{c_4} \emptyset \end{aligned}\right\} \tag{34}$$

The state-change vectors for these four reactions are

$$\left.\begin{aligned} \boldsymbol{\nu}_1 &= (1, 0) \\ \boldsymbol{\nu}_2 &= (-1, 1) \\ \boldsymbol{\nu}_3 &= (1, -1) \\ \boldsymbol{\nu}_4 &= (-1, 0) \end{aligned}\right\} \tag{35a}$$

and the corresponding propensity functions are

$$\left.\begin{aligned} a_1(\boldsymbol{x}) &= k_1\Omega \\ a_2(\boldsymbol{x}) &= c_2 x_1 \\ a_3(\boldsymbol{x}) &= k_3\Omega^{-2}\tfrac{1}{2}x_1(x_1 - 1)x_2 \\ a_4(\boldsymbol{x}) &= c_4 x_1 \end{aligned}\right\} \tag{35b}$$

The Ω-independent functions defined in (8) are therefore

$$\left.\begin{aligned} \tilde{a}_1(\boldsymbol{z}) &= k_1 \\ \tilde{a}_2(\boldsymbol{z}) &= c_2 z_1 \\ \tilde{a}_3(\boldsymbol{z}) &= k_3\tfrac{1}{2}z_1^2 z_2 \\ \tilde{a}_4(\boldsymbol{z}) &= c_4 z_1 \end{aligned}\right\} \tag{35c}$$

We take values for the rate constants which put the Brusselator in a limit-cycle regime

$$k_1 = 5000, \quad c_2 = 50, \quad k_3 = 5 \times 10^{-5}, \quad c_4 = 5 \tag{36a}$$

For the initial condition, we take

$$X_1(0) = 1001 \cdot \Omega, \quad X_2(0) = 2002 \cdot \Omega \tag{36b}$$

which is slightly off of the equilibrium point.

Fig. 5 shows for the case $\Omega = 1$ the one-standard deviation envelope for $Z_1(t)$ over the time interval $0 \le t \le 4$ as predicted by the LNA (dotted curves) and the SSA (solid and dashed curves), the latter again being computed from 10^5 runs. The grey jagged curve is the $Z_1(t)$ trajectory of a typical one of those SSA runs. The performance of the LNA in this case is obviously not good. Although the RRE trajectory $\hat{Z}_1(t)$ (the heavy dotted curve) gives a reasonable representation of the behaviour of the single-run SSA trajectory, except for an overall shift in phase, the LNA's estimate of the standard deviation about $\hat{Z}_1(t)$ (lightly dotted curve) is extremely poor. The upper one-

doi: 10.1049/iet-syb.2011.0038

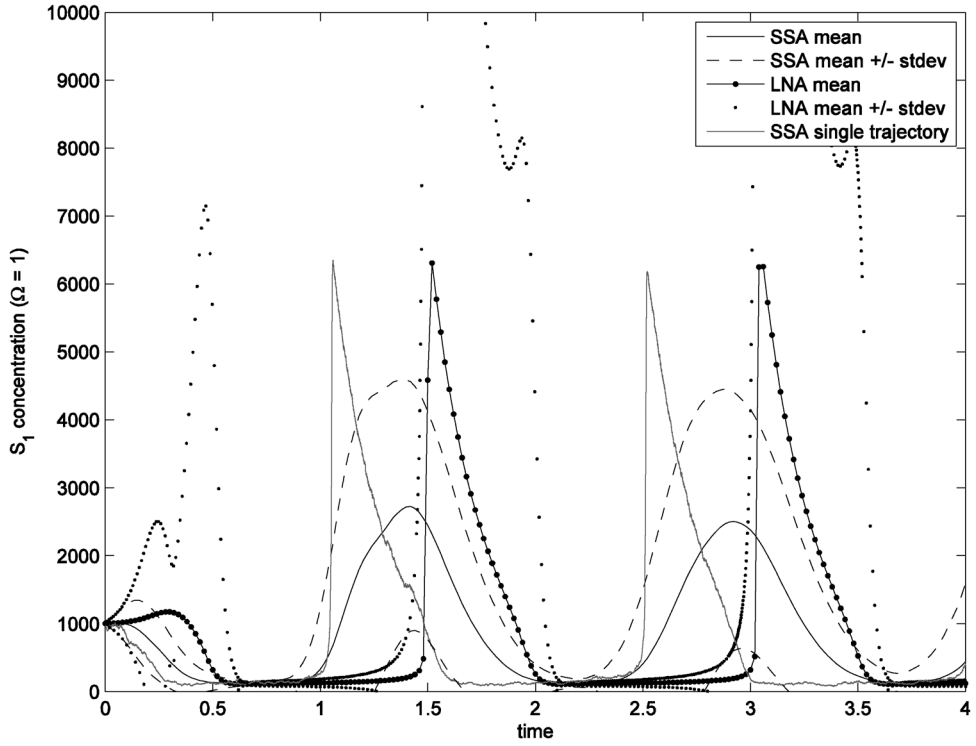

Fig. 5 *Brusselator model in (34)–(36) for $\Omega = 1$: mean and mean $\pm$ one-standard deviation of the concentration of species S_1 as computed from 10^5 SSA simulations (solid and dashed curves) and from the LNA (dotted curves)*

Jagged grey curve is a typical SSA trajectory for species S_1; it shows that although the S_1 population sometimes rises to over 6000, for much of the time it is well under 200. The inaccuracy of the LNA for this 'small' limit-cycle system over this time frame is mainly because of the cumulative effects of the fluctuations in the phase of the oscillator

standard deviation envelope predicted by the LNA in the last oscillation peaks at about 9×10^5, and that peak value would become even larger if the run had contained more oscillations.

Fig. 6 shows the results obtained if these calculations are repeated with the volume increased to $\Omega = 10^5$. Here, the SSA prediction consists of only one simulated trajectory, because the SSA trajectories at this high molecular

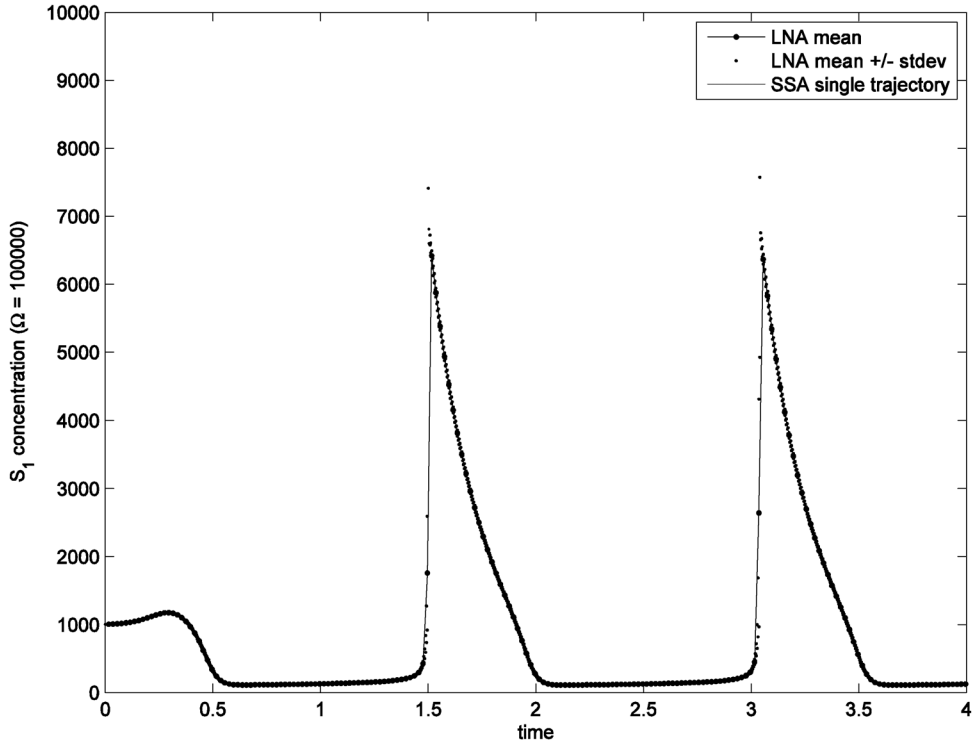

Fig. 6 *Same as Fig. 5, but with $\Omega = 10^5$: moving closer to the thermodynamic limit allows the LNA to give a much more accurate approximation over the same time frame*

But over longer time frames, the performance of the LNA would again deteriorate for this limit-cycle oscillator

population level take a very long time to compute and the trajectories were found to be practically indistinguishable from each other over this span of time. We see that at least up to time $t = 4$, the SSA trajectory is well predicted by the LNA's very tight one-standard deviation envelope. However, we can see evidence of a gradually increasing instability in the LNA's one-standard deviation envelope at the peaks of the last two oscillations. If this plot had been extended to many more oscillations, these overestimates would eventually become as wildly inaccurate as the LNA estimates in Fig. 5. However, if the oscillating system is sufficiently large, the LNA will accurately describe its behaviour over a sufficiently restricted time span.

This picture is consistent with recent work applying the LNA to chemical oscillators by Boland *et al.* [36] and Scott [37]. They separated the fluctuations into components normal and tangential to the limit cycle trajectory by adopting a rotating coordinate frame in the plane of the Brusselator's limit cycle, obtained from the RRE. One obtains an LNA variance for the normal component that is accurate for moderate molecular populations. However, as discussed in Section 1, the tangential fluctuations, which are essentially fluctuations in the phase of the limit cycle oscillations, grow unboundedly. This unbounded growth in the phase fluctuations is responsible for the unruly behaviour shown in Fig. 5 of the standard LNA for moderate population sizes.

7 Summary

We have shown that if a well-stirred chemically reacting system is sufficiently close to the thermodynamic limit, the limit in which the system volume Ω and the molecular populations $\boldsymbol{X}(t)$ are infinitely large but the molecular concentrations $\boldsymbol{Z}(t) \equiv \boldsymbol{X}(t)/\Omega$ are finite, the system's time evolution will be accurately described by the CLE (9), at least for a limited span of time. The CLE's duration of validity will be longer for some systems than others (e.g. longer for a monostable system than a bistable system or an oscillating system), but it can always be made as long as desired simply by taking the system close enough to the thermodynamic limit. We have further shown that in the full thermodynamic limit, the CLE becomes the traditional deterministic RRE (10), in which that infinite-size limit will be valid for an effectively infinite span of time. We have arrived at these conclusions without invoking the sometimes problematic system-size expansion of van Kampen, and also without making an arbitrary truncation of the Kramers-Moyal expansion of the CME.

Against this background, we then showed that the LNA in (11) and (17) can be derived with relative ease as a linearised approximation of the CLE. This way of deriving the LNA makes it clear that the LNA shares the CLE's requirements for validity, a conclusion that we substantiated in the numerical examples in Section 6. This way of deriving the LNA also suggests that it would be more accurate to view the LNA as an approximation of the CLE, and only indirectly as an approximation of the CME. This view is consistent with Gardiner's derivation of the LNA as a linearisation of the two-term-truncated Kramers-Moyal equation, as that truncated equation is mathematically equivalent to the CLE. This view is also in line with the more recent findings of Grima *et al.* [21] that the Fokker-Planck equation corresponding to the CLE is more accurate than the LNA.

As the LNA is an approximation of the CLE, and the CLE becomes the RRE in the thermodynamic limit, what the LNA gives us in practical terms is a description of the 'initial stochastic departure' of the CLE from the RRE as we back away from the thermodynamic limit to a finite but still large system. More specifically, the LNA tells us that that initial departure from the purely deterministic RRE behaviour consists of normal fluctuations in the concentration $\boldsymbol{Z}(t)$ about the deterministic RRE concentration $\hat{\boldsymbol{Z}}(t)$ with $\mathrm{var}\{Z_i(t)\} = \Omega^{-1}\kappa_{ii}(t)$, where $\kappa_{ij}(t)$ is the solution of the ordinary differential equation set (21) subject to the initial condition (22).

For $i \neq j$, $\Omega^{-1}\kappa_{ij}(t)$ is the covariance of the molecular concentrations of species S_i and S_j. The corresponding correlation in (26), which is a more accurate indicator of pairwise correlations (the covariance in some cases behaves oppositely to the correlation), is therefore independent of Ω. That means that the pairwise correlations between species concentrations in the stochastic LNA regime carry over unchanged into the deterministic thermodynamic limit, where the variances and covariances vanish. In other words, the correlations predicted by the stochastic LNA are in some sense equally present in the deterministic RRE.

We emphasise that, unlike earlier studies of the validity of the LNA, our conclusions here are not restricted to specially chosen systems. We have shown quite generally that the LNA will serve in the manner described above for all realistic systems which are sufficiently large, although in some cases for only a limited span of time.

8 Acknowledgments

The authors thank the reviewers for some very beneficial comments, and E.W. also thank Marc Benayoun for helpful discussions. They also acknowledge financial support as follows: D.G. was supported by the California Institute of Technology through Consulting Agreement No. 102-1080890 pursuant to Grant No. R01GM078992 from the National Institute of General Medical Sciences, and through Contract No. 82-1083250 pursuant to Grant No. R01EB007511 from the National Institute of Biomedical Imaging and Bioengineering, and also from the University of California at Santa Barbara under Consulting Agreement No. 054281A20 pursuant to funding from the National Institutes of Health. K.S. and L.P. were supported by Grant No. R01EB007511 from the National Institute of Biomedical Imaging and Bioengineering, DOE Contract No. DE-FG02-04ER25621, NSF Contract No. IGERT DG02-21715, and the Institute for Collaborative Biotechnologies through Grant No. DFR3A-8-447850-23002 from the US Army Research Office. K.S. was also supported by a National Science Foundation Graduate Research Fellowship.

9 References

1 Kurtz, T.G.: 'The relationship between stochastic and deterministic models for chemical reactions', *J. Chem. Phys.*, 1972, **57**, pp. 2976–2978
2 Kurtz, T.G.: 'Limit theorems and diffusion approximations for density dependent Markov chains', *Math. Program. Stud.*, 1976, **5**, pp. 67–78
3 Kurtz, T.G.: 'Strong approximation theorems for density dependent Markov chains', *Stoch. Process. Appl.*, 1978, **6**, pp. 233–240
4 van Kampen, N.G.: 'The expansion of the master equation', *Adv. Chem. Phys.*, 1976, **34**, pp. 245–309
5 van Kampen, N.G.: 'Stochastic processes in physics and chemistry' (North-Holland, 1992)

doi: 10.1049/iet-syb.2011.0038

6 Gardiner, C.W.: 'Handbook of stochastic methods for physics, chemistry and the natural sciences' (Springer-Verlag, 1985)
7 Gillespie, D.T.: 'The deterministic limit of stochastic chemical kinetics', *J. Phys. Chem. B*, 2009, **113**, pp. 1640–1644
8 Lefever, R., Nicolis, G.: 'Chemical instabilities and sustained oscillations', *J. Theor. Biol.*, 1971, **30**, pp. 267–284
9 Nicolis, G.: 'Stability and dissipative structures in open systems far from equilibrium', *Adv. Chem. Phys.*, 1971, **19**, pp. 209–324
10 Wallace, E., Benayoun, M., van Drongelen, W., Cowan, J.D.: 'Emergent oscillations in networks of stochastic spiking neurons', PLoS ONE, 2011, 6, article id e14804
11 Elf, J., Paulsson, J., Berg, O.G., Ehrenberg, M.: 'Near-critical phenomena in intracellular metabolite pools', *Biophys. J.*, 2003, **84**, pp. 154–170
12 Bressloff, P.C.: 'Metastable states and quasicycles in a stochastic Wilson-Cowan model of neuronal population dynamics', *Phys. Rev. E*, 2010, **82**, article id 051903
13 Benayoun, M., Cowan, J.D., van Drongelen, W., Wallace, E.: 'Avalanches in a stochastic model of spiking neurons', *PLoS Comput. Biol.*, 2010, **6**, article id e1000846
14 McKane, A.J., Nagy, J.D., Newman, T.J., Stefanini, M.O.: 'Amplified biochemical oscillations in cellular systems', *J. Stat. Phys.*, 2007, **128**, pp. 165–191
15 Dauxois, T., Di Patti, F., Fanelli, D., McKane, A.J.: 'Enhanced stochastic oscillations in autocatalytic reactions', *Phys. Rev. E*, 2009, **79**, article id 036112
16 McKane, A.J., Newman, T.J.: 'Predator-prey cycles from resonant amplification of demographic stochasticity', *Phys. Rev. Lett.*, 2005, **94**, article id 218102
17 Grima, R.: 'Noise-induced breakdown of the Michaelis-Menten equation in steady-state conditions', *Phys. Rev. Lett.*, 2009, **102**, article id 218103
18 Grima, R.: 'Investigating the robustness of the classical enzyme kinetic equations in small intracellular compartments', *BMC Sys. Biol.*, 2009, **3**, p. 101
19 Grima, R.: 'An effective rate equation approach to reaction kinetics in small volumes: theory and application to biochemical reactions in nonequilibrium steady-state conditions', *J. Chem. Phys.*, 2010, **133**, article id 035101
20 Thomas, P., Straube, A.V., Grima, R.: 'Stochastic theory of large-scale enzyme-reaction networks: finite copy number corrections to rate equation models', *J. Chem. Phys.*, 2010, **133**, article id 195101
21 Grima, R., Thomas, P., Straube, A.V.: 'How accurate are the nonlinear chemical Fokker-Planck and chemical Langevin equations?', *J. Chem. Phys.*, 2011, **135**, article id 084103
22 Cianci, C., Di Patti, F., Fanelli, D., Barletti, L.: 'Analytical study of non Guassian fluctuations in a stochastic scheme of autocatalytic reactions'. arXiv:1104.5668v1 [cond-mat.stat-mech]
23 Cianci, C., Di Patti, F., Fanelli, D.: 'Non-Gaussian fluctuations in stochastic models with absorbing barriers'. arXiv:1104.5570v1 [cond-mat.stat-mech]
24 Ferm, L., Lötstedt, P., Hellander, A.: 'A hierarchy of approximations of the master equation scaled by a size parameter', *J. Sci. Comput.*, 2008, **34**, pp. 127–151
25 Gillespie, D.T.: 'A diffusional bimolecular diffusion function', *J. Chem. Phys.*, 2009, **131**, article id 164109
26 McQuarrie, D.A.: 'Stochastic approach to chemical kinetics', *J. Appl. Prob.*, 1967, **4**, pp. 413–487
27 Gillespie, D.T.: 'A general method for numerically simulating the stochastic time evolution of coupled chemical reactions', *J. Comput. Phys.*, 1976, **22**, pp. 403–434
28 Gillespie, D.T.: 'Exact stochastic simulation of coupled chemical reactions', *J. Phys. Chem.*, 1977, **81**, pp. 2340–2361
29 Gillespie, D.T.: 'Approximate accelerated stochastic simulation of chemically reacting systems', *J. Chem. Phys.*, 2001, **115**, pp. 1716–1733
30 Cao, Y., Gillespie, D.T., Petzold, L.R.: 'Efficient stepsize selection for the tau-leaping simulation method', *J. Chem. Phys.*, 2006, **124**, article id 044109
31 Gillespie, D.T.: 'The chemical Langevin equation', *J. Chem. Phys.*, 2000, **113**, pp. 297–306
32 Gillespie, D.T.: 'The chemical Langevin and Fokker-Planck equations for the reversible isomerization reaction', *J. Phys. Chem. A*, 2002, **106**, pp. 5063–5071
33 Gillespie, D.T.: 'Stochastic simulation of chemical kinetics', *Ann. Rev. Phys. Chem.*, 2007, **58**, pp. 35–55
34 Sanft, K.R., Wu, S., Roh, M., Fu, J., Lim, R.K., Petzold, L.R.: 'StochKit2: Software for discrete stochastic simulation of biochemical systems with events', *Bioinformatics*, 2011, **27**, pp. 2457–2458
35 Hindmarsh, A.C., Brown, P.N., Grant, K.E., *et al.*: 'SUNDIALS: suite of nonlinear and differential/algebraic equation solvers', *ACM Trans. Math. Soft.*, 2005, **31**, (3), pp. 363–396
36 Boland, R.P., Galla, T., McKane, A.J.: 'Limit cycles, complex Floquet multipliers, and intrinsic noise', *Phys. Rev. E*, 2009, **79**, article id 051131
37 Scott, M.: 'Applied stochastic processes in science and engineering' 2011, Internet posting at http://www.math.uwaterloo.ca/~mscott/Notes.pdf

10 Appendix: solving the LNA

Writing the LNA (17) in its component form

$$\xi_i(t+\mathrm{d}t) \doteq \xi_i(t) + \sum_{k=1}^{N}\left(\sum_{m=1}^{M}\nu_{im}f_{mk}(t)\right)\xi_k(t)\,\mathrm{d}t + \sum_{m=1}^{M}\nu_{im}\sqrt{\tilde{a}_m(\hat{\boldsymbol{Z}}(t))}\,N_m(t)\sqrt{\mathrm{d}t} \quad (i=1,\ \ldots,N) \tag{37}$$

we will first prove that the $\xi_i(t)$ defined by this equation are all normal random variables. The key to doing that is a result in random variable theory which states that if Y_1 and Y_2 are two normal random variables, and c_1 and c_2 are two sure (non-random) variables, then $c_1Y_1 + c_2Y_2$ is a normal random variable. This is true even if Y_1 and Y_2 are statistically dependent. Therefore as $\xi_i(t_0) = 0 = \mathcal{N}(0, 0)$ and $N_m(t_0) = \mathcal{N}(0, 1)$, we may conclude from the $t = t_0$ version of (37) that $\xi_i(t_0 + \mathrm{d}t)$ is a normal random variable – because the coefficients of both $\xi_k(t)$ and $N_m(t)$ on the right side of (37) are sure variables. The same reasoning applied to the $t = t_0 + \mathrm{d}t_0$ version of (37) then establishes that $\xi_i(t_0 + 2\mathrm{d}t)$ is a normal random variable. By induction, we conclude that $\xi_i(t)$ is normal for all $t > t_0$. (It should be noted that the foregoing logic cannot be applied to the LNA's precursor (14), because in that equation the coefficient of $N_m(t)$ on the right side is not a sure variable; or from a different point of view, that cannot be done because the product of a normal random variable with practically any other random variable will not be normal. Nor can we in those other cases invoke the central limit theorem to infer normality for the sum of 'infinitely many terms', because those terms are not statistically independent.) The N normal random variables $\xi_1(t), \ldots, \xi_N(t)$ will usually not be statistically independent; however, being normal, they will be completely specified by their N means and their $N(N-1)/2$ covariances.

To prove that the normal random variables $\xi_i(t)$ have zero mean, we first take the average of (37)

$$\langle\xi_i(t+\mathrm{d}t)\rangle \doteq \langle\xi_i(t)\rangle + \sum_{k=1}^{N}\left(\sum_{m=1}^{M}\nu_{im}f_{mk}(t)\right)\langle\xi_k(t)\rangle\,\mathrm{d}t + \sum_{m=1}^{M}\nu_{im}\sqrt{\tilde{a}_m(\hat{\boldsymbol{Z}}(t))}\langle N_m(t)\rangle\sqrt{\mathrm{d}t} \quad (i=1,\ldots,N)$$

As $\langle N_m(t)\rangle = 0$, this reduces to the set of coupled ordinary differential equations

$$\frac{\mathrm{d}\langle\xi_i(t)\rangle}{\mathrm{d}t} \doteq \sum_{k=1}^{N}\left(\sum_{m=1}^{M}\nu_{im}f_{mk}(t)\right)\langle\xi_k(t)\rangle \quad (i=1,\ \ldots,N) \tag{38}$$

Equation 18 implies the initial condition $\langle \xi_i(t) \rangle = 0$ for all i. However, $\langle \xi_i(t) \rangle \equiv 0$ is a solution of (38) which satisfies that initial condition; hence, for all $t \geq t_0$

$$\langle \xi_i(t) \rangle \equiv 0 \quad (i = 1, \ldots, N) \tag{39}$$

To derive a formula for the time derivative of $\kappa_{ij}(t) \equiv \langle \xi_i(t) \xi_j(t) \rangle$, we multiply (37) by itself with i replaced by j. Retaining only terms up to first order in $\mathrm{d}t$, that gives

$$\begin{aligned}
\xi_i(t + \mathrm{d}t)\, \xi_j(t + \mathrm{d}t) \doteq\ & \xi_i(t) \xi_j(t) \\
& + \sum_{k=1}^{N} \left(\sum_{m=1}^{M} \nu_{im} f_{mk}(t) \right) \xi_k(t)\, \xi_j(t)\, \mathrm{d}t \\
& + \sum_{k=1}^{N} \left(\sum_{m=1}^{M} \nu_{jm} f_{mk}(t) \right) \xi_k(t)\, \xi_i(t)\, \mathrm{d}t \\
& + \sum_{m=1}^{M} \nu_{im} \sqrt{\tilde{a}_m(\hat{\boldsymbol{Z}}(t))}\, N_m(t) \xi_j(t) \sqrt{\mathrm{d}t} \\
& + \sum_{m=1}^{M} \nu_{jm} \sqrt{\tilde{a}_m(\hat{\boldsymbol{Z}}(t))}\, N_m(t) \xi_i(t) \sqrt{\mathrm{d}t} \\
& + \sum_{m=1}^{M} \nu_{im} \sqrt{\tilde{a}_m(\hat{\boldsymbol{Z}}(t))}\, N_m(t) \sum_{l=1}^{M} \nu_{jl} \sqrt{\tilde{a}_l(\hat{\boldsymbol{Z}}(t))}\, N_l(t)\, \mathrm{d}t
\end{aligned}$$

Averaging this equation, using

$$\langle N_m(t) \xi_i(t) \rangle = \langle N_m(t) \rangle \langle \xi_i(t) \rangle = 0$$

and

$$\langle N_m(t) N_l(t) \rangle = \begin{cases} 1, \text{ if } l = m \\ 0, \text{ if } l \neq m \end{cases}$$

we obtain

$$\begin{aligned}
\langle \xi_i(t + \mathrm{d}t)\, \xi_j(t + \mathrm{d}t) \rangle \doteq\ & \langle \xi_i(t) \xi_j(t) \rangle \\
& + \sum_{k=1}^{N} \left(\sum_{m=1}^{M} \nu_{im} f_{mk}(t) \right) \langle \xi_k(t) \xi_j(t) \rangle\, \mathrm{d}t \\
& + \sum_{k=1}^{N} \left(\sum_{m=1}^{M} \nu_{jm} f_{mk}(t) \right) \langle \xi_k(t) \xi_i(t) \rangle\, \mathrm{d}t \\
& + \sum_{m=1}^{M} \nu_{im} \nu_{jm}\, \tilde{a}_m(\hat{\boldsymbol{Z}}(t))\, \mathrm{d}t
\end{aligned} \tag{40}$$

Transposing the first term on the right side, dividing through by $\mathrm{d}t$, and finally taking the limit $\mathrm{d}t \to 0$, we obtain (21).

doi: 10.1049/iet-syb.2011.0038